

**Goos-Hänchen effect in light transmission through biperiodic photonic-magnonic crystals**Yu. S. Dadoenkova,<sup>1,2,3</sup> N. N. Dadoenkova,<sup>2,3</sup> J. W. Klos,<sup>4</sup> M. Krawczyk,<sup>4</sup> and I. L. Lyubchanskii<sup>3</sup><sup>1</sup>*Institute of Electronics and Information Systems, Novgorod State University, 173003 Veliky Novgorod, Russian Federation*<sup>2</sup>*Ulyanovsk State University, 432017 Ulyanovsk, Russian Federation*<sup>3</sup>*Donetsk Physical and Technical Institute of the National Academy of Sciences of Ukraine, Ukraine*<sup>4</sup>*Faculty of Physics, Adam Mickiewicz University in Poznań, 61-614 Poznań, Poland*

(Received 10 April 2017; published 2 October 2017)

We present a theoretical investigation of the Goos-Hänchen effect, i.e., the lateral shift of the light beam transmitted through one-dimensional biperiodic multilayered photonic systems consisting of equidistant magnetic layers separated by finite size dielectric photonic crystals. We show that the increase of the number of periods in the photonic-magnonic structure leads to increase of the Goos-Hänchen shift in the vicinity of the frequencies of defect modes located inside the photonic band gaps. Presence of the linear magnetoelectric coupling in the magnetic layers can result in a vanishing of the positive maxima of the cross-polarized contribution to the Goos-Hänchen shift.

DOI: [10.1103/PhysRevA.96.043804](https://doi.org/10.1103/PhysRevA.96.043804)**I. INTRODUCTION**

The Goos-Hänchen effect consists of the lateral shift of a reflected light beam with respect to the prediction of geometric optics [1]. Nowadays, this effect is intensively studied [2–7] in different systems, including anisotropic crystals and magnetic materials [8–16], graphene [4,17–19], superconductors [20,21], and photonic crystals (PCs) [22–25], despite the long history of investigations since the first observation of this phenomenon in 1947 [1]. Some aspects of the Goos-Hänchen effect were studied in different structures (see, for example, recent review papers [26,27]). The Goos-Hänchen shift (GHS) of partially coherent light in epsilon-near-zero metamaterials was theoretically investigated in [28]. A giant GHS (up to 70 wavelengths) and an angular shift of several hundred microradians were observed in two-dimensional (2D) metasurfaces composed of PMMA gratings on a gold surface [29]. Giant GHS has been predicted also for spin waves in magnetic films [30–33], and optical phonons [34]. This phenomenon has potential application in designing integrated optics devices, such as optical switchers and bio- and chemical sensors and detectors [35–39].

The GHS in multilayered systems can exhibit interesting peculiarities. For instance, giant GHSs are experimentally demonstrated from a prism-coupled PC structure through a band-gap-enhanced total internal reflection [40]. All-optical tunability of the GHS in PCs was demonstrated in [41]. The lateral shift of the reflected beam can be remarkably enhanced when the phase-matching conditions are satisfied for the surface polariton excitation at the interface of the structure in the graphene-induced photonic band gap (PBG) [42]. The GHS reversibility near the band-crossing structure of PCs containing left-handed metamaterials was shown in [43]. The GHS at the PBG edges can reach values up to several hundreds of wavelengths [44]. Similarly, when a light beam is incident on a PC containing a defect layer, the GHSs are greatly enhanced near the defect mode due to the electromagnetic wave localization [45]. On the contrary, in  $\mathcal{PT}$ -symmetric crystals the GHS can be huge inside the reflection band [46,47]. The following biperiodic structures are also of potential interest: photonic-magnonic crystals (PMCs)

which provide PBGs in the spectra of electromagnetic waves and magnonic band gaps in spin wave spectra [48–50], and photonic hypercrystals [51].

In this paper, we investigate the GHS of light in one-dimensional biperiodic PMCs. The photonic spectra of such PMCs are characterized by narrow inside-band-gap modes with fine structure [48–50], and it would be expected that the GHS could reach large values in the vicinity of these modes. We take into account magnetoelectric properties of the magnetic layers because they can provide important influence on the electromagnetic wave propagation [52].

**II. MODEL AND METHOD OF GOOS-HÄNCHEN SHIFT CALCULATION**

We consider PMCs consisting of magnetic layers  $M$  of thickness  $d_M$  separated by nonmagnetic dielectric spacers composed of alternating layers  $A$  and  $B$  of thicknesses  $d_A$  and  $d_B$ , respectively, as illustrated in Fig. 1. The magnetic layers are magnetically saturated with the magnetization vector  $\mathbf{M}$  lying in the incidence plane and parallel to the interfaces (longitudinal magneto-optical configuration). As a reference structure, we investigate ABA, three layers placed between two magnetic films  $M$  [the structure  $M(ABA)M$ , Fig. 1(a)]. Then we increase the number  $N$  of dielectric unit cells (AB) in the nonmagnetic spacer and consider it as a PC of structure  $(AB)^N A$  of thickness  $d_d = N(d_A + d_B) + d_A$ . The magnetic supercell  $[M(AB)^N A]$  is repeated  $K$  times [Fig. 1(b)], so that the structure  $[M(AB)^N A]^K M$  is a biperiodic PMC [48–50]. We assume a light beam of the angular frequency  $\omega$  is incident under angle  $\theta$  from vacuum [with  $(xz)$  being the incidence plane] and at the transmission trough the structure undergoes a lateral shift  $\Delta L$ . A specific class of magnetic materials possesses spontaneous magnetoelectric properties [52]. The magnetoelectric effect consisting of a magnetization induction by an electric field and a dielectric polarization induction by a magnetic field was observed in many systems, including magnetic garnets [53,54]. This effect increases the cross-polarized contribution to the light reflected from



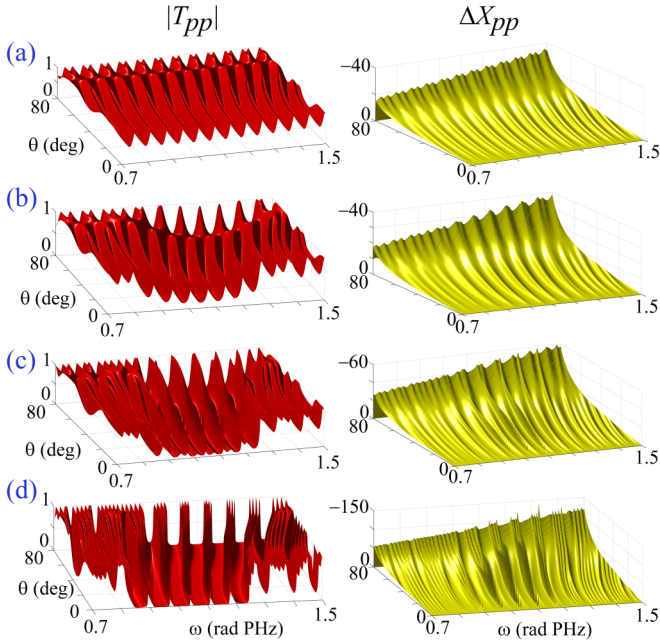


FIG. 2. Transmission coefficient  $|T_{pp}|$  and the corresponding dimensionless GHS  $\Delta X_{pp}$  as functions of the angular frequency  $\omega$  and incidence angle  $\theta$  for the structures (a) M(ABA)M; (b) M(AB)<sup>4</sup>AM; (c) [M(AB)<sup>4</sup>A]<sup>2</sup>M; (d) [M(AB)<sup>4</sup>A]<sup>5</sup>M.

the layers can be distorted. However, a slight change in the thicknesses of the films will not change the behavior of the transmittivity and lateral shifts significantly. This would only lead to a slight drift of the frequency positions of the inside-band-gap modes and PBG edges.

We consider an incident Gaussian beam with waist  $w_0 = 30 \mu\text{m}$ . In this case the impact of the second term in Eq. (4) on the GHS experienced by the transmitted beam is about 5% in the vicinity of the PBG edges and inside-band-gap modes.

### A. Transmittivity and Goos-Hänchen shift spectra

The transmission spectra  $|T_{pp}|$ ,  $|T_{ss}|$ , and  $|T_{ps}| = |T_{sp}|$  and the corresponding GHSs  $\Delta X_{pp}$ ,  $\Delta X_{ss}$ , and  $\Delta X_{ps} = \Delta X_{sp}$  are presented in the left and right panels of Figs. 2–4, respectively, for different photonic structures (see Fig. 1). Here we neglect the magnetoelectric coupling in the YIG layers, so that  $\alpha = 0$ .

The transmission spectra of the system M(ABA)M [see Fig. 1(a)] demonstrate the stripe structure of the minima and maxima. The values of the diagonal transmission matrix components  $|T_{pp}|$  and  $|T_{ss}|$  [Figs. 2(a) and 3(a)] vary from 0.1 to 1, while the maxima of the off-diagonal component  $|T_{ps}|$  do not exceed  $3 \times 10^{-3}$  [Fig. 4(a)]. The corresponding GHSs are negative. The diagonal shift  $\Delta X_{pp}$  is about several wavelengths for the incidence angles  $\theta < 60^\circ$ , and its values slowly vary according to the minima and maxima of  $T_{pp}$ , though this variation is about a few  $\lambda$  [see Fig. 2(a)]. At  $\theta > 60^\circ$ ,  $\Delta X_{pp}$  increases in absolute value up to four tens of  $\lambda$ . For the fixed  $\theta$ , the values of  $\Delta X_{pp}$  increase with the increase of the frequency  $\omega$ . The GHSs  $\Delta X_{ss}$  and  $\Delta X_{ps}$  demonstrate similar tendencies to that for  $\Delta X_{pp}$  at  $\theta < 60^\circ$ , but at  $\theta > 60^\circ$  have more pronounced difference in minima

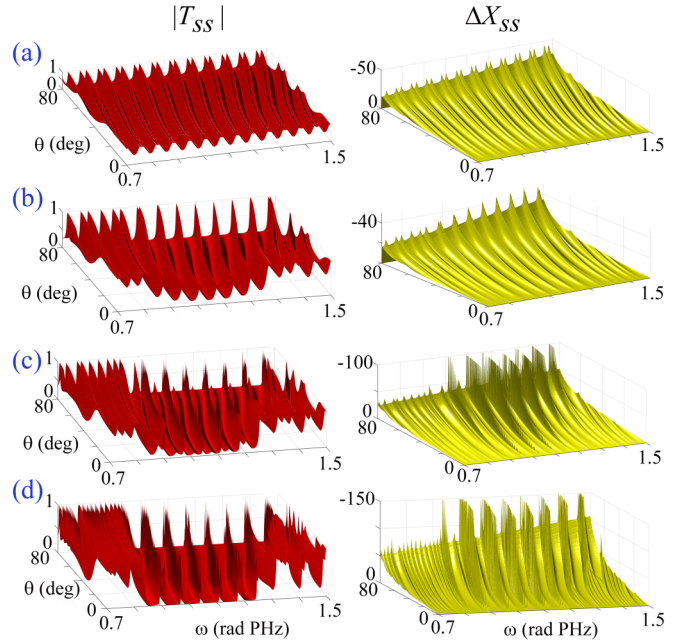


FIG. 3. The same as in Fig. 2 except for  $|T_{ss}|$  and  $\Delta X_{ss}$ .

and maxima because the variation of  $T_{ss}$  and  $T_{ps}$  (as well as their phases) responsible for the GHS [Eq. (1)] is higher.

Further addition of (AB) bilayers between the magnetic layers M leads to appearance of the PBG in the transmission spectra. The left (right) panels in Figs. 2(b), 3(b), and 4(b) show  $|T_{pp}|$ ,  $|T_{ss}|$ , and  $|T_{ps}|$  ( $\Delta X_{pp}$ ,  $\Delta X_{ss}$ , and  $\Delta X_{ps}$ ) for the system [M(AB)<sup>N</sup>A]<sup>K</sup>M with  $N = 4$  dielectric cells and  $K = 1$  magnetic supercell, so that this structure presents a dielectric PC with two defect layers M. A set of wide and equidistantly distributed defect modes appears in the PBGs spectra. These modes shift towards higher  $\omega$  with the increase

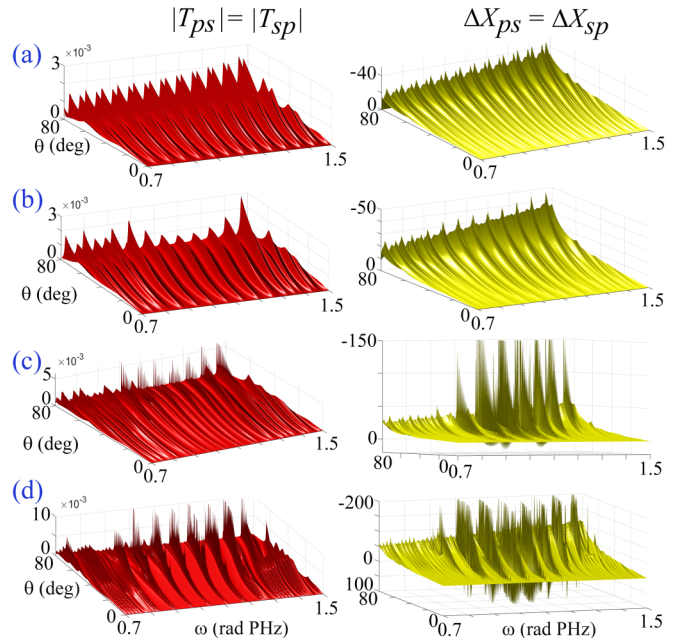


FIG. 4. The same as in Fig. 2 except for  $|T_{ps}| = |T_{sp}|$  and  $\Delta X_{ps} = \Delta X_{sp}$ .

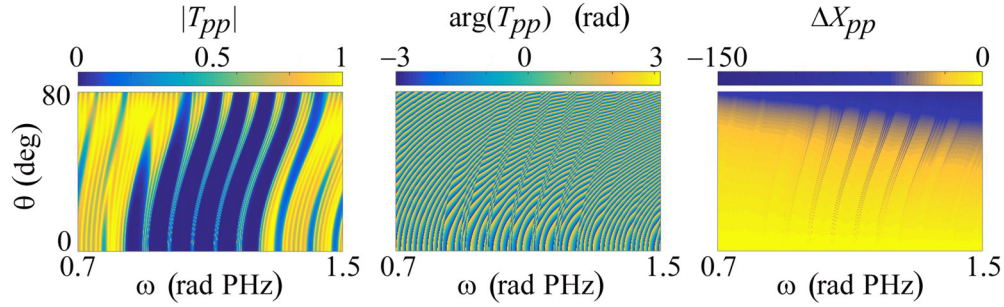


FIG. 5. Color maps of the evolution of the transmittivity  $|T_{pp}|$ , its phase  $\arg(T_{pp})$ , and GHS  $\Delta X_{pp}$  with the angular frequency  $\omega$  and incidence angle  $\theta$  for the PMC of the structure  $[M(AB)^4A]^5M$ .

of  $\theta$  for all polarization states. In the case of  $T_{pp}$ , the defect modes merge at  $\theta \approx 60^\circ$ , and the PBG shrinks [Fig. 2(b)]. On the contrary, the widths of the PBGs in the spectra of  $T_{ss}$  and  $T_{ps}$  increase with  $\theta$ , as shown in Figs. 3(b) and 4(b), respectively. Variation of the GHSs at the frequencies inside the PBGs becomes more pronounced relative to the structure  $M(ABA)M$  with a single dielectric period, as follows from comparison of Figs. 2(a), 3(a), and 4(a) with 2(b), 3(b), and 4(b). Frequency positions of the negative maxima of  $\Delta X_{ij}$  correspond to the defect mode positions.

Figures 2(c), 3(c), and 4(c) show results for the structure  $[M(AB)^4A]^K M$  with  $K = 2$  magnetic supercells. This structure can be treated as a dielectric PC with three magnetic defect layers  $M$ . The defect modes in the PBGs spectra overall become narrower and at high  $\theta$  do not merge anymore in the  $T_{pp}$  spectrum. The values of the defect mode maxima of  $T_{ps}$  are larger than for the previously described structures, as one can see from comparison of Figs. 4(a), 4(b), and 4(c). The negative maxima of the corresponding GHSs increase and can reach values of about  $-100\lambda$  even at low  $\theta$ .

With the extension of the structure by increasing the number  $K$  of supercell  $[M(AB)^4A]$ , the magnetophotonic structure can be considered as a PMC with biperiodicity: a magnetic and a dielectric ones with the periods  $d_M + d_d$  and  $d_A + d_B$ , respectively. The PBG is still formed due to the dielectric PCs  $(AB)^4$ , and repetition of the magnetic supercells leads to forming the inside-band-gap modes of high transmittivity. This is illustrated in Figs. 2(d), 3(d), and 4(d) for the PMC with  $K = 5$  magnetic supercells. The positions of the inside-band-gap modes of  $T_{pp}$ ,  $T_{ss}$ , and  $T_{ps}$  coincide only at normal incidence. The intensity of the inside-band-gap modes in  $T_{ps}$  spectra is higher than in the previously discussed structures. Moreover, outside the PBG the values of  $|T_{ps}|$  increase with  $K$  up to  $10^{-2}$  [Figs. 4(a) and 4(d)]. The negative maxima of the GHSs which correspond to the inside-band-gap modes can reach values up to  $-200\lambda$  [Fig. 4(d)]. However, the peaks of GHS for  $s$ - $s$  and  $p$ - $s$  ( $s$ - $p$ ) transmission ( $\Delta X_{ss}$  and  $\Delta X_{ps}$ ) are sharper and reach values higher than for  $p$ - $p$  transmission ( $\Delta X_{pp}$ ). It should be noted that  $\Delta X_{ps}$  in PMCs with  $K \geq 2$  possesses positive values at some inside-band-gap mode frequencies [Figs. 4(c) and 4(d)]. The increase of the GHSs around the inside-band-gap mode positions is caused by abrupt change of the transmission coefficient's both absolute value and phase. This can be seen from Fig. 5 which shows color maps of the transmittivity  $|T_{pp}|$ , its phase  $\arg(T_{pp})$ , and GHS  $\Delta X_{pp}$  evolution with the angular frequency  $\omega$  and incidence angle  $\theta$  for the case of  $p$ - $p$

transmission. As was mentioned above, the impact of the second term of Eq. (4) on the calculated GHS does not exceed 5%. Thus the GHS values are mostly provided by the phase variation. Indeed, as Figs. 5(a) and 5(b) show, in the vicinity of the inside-band-gap modes the phase of the transmission coefficient exhibits abrupt change that results in large GHS, illustrated in Fig. 5(c). This behavior is similar for all polarization combinations of the incident and transmitted light.

## B. Magnetolectric effect influence on the Goos-Hänchen shift in the vicinity of the inside-band-gap mode

As was shown in [48–50], the inside-band-gap modes in the transmittivity spectra of a biperiodic PMC possess a fine structure, and the number of subpeaks is related to the number of magnetic supercells. In Fig. 6 we show the influence of the magnetolectric interaction on properties of the light transmitted through the PMC of the structure  $[M(AB)^4A]^5M$ , focusing on the details of a single inside-band-gap mode for  $\theta = 30^\circ$ . The solid lines correspond to the previously studied case when no magnetolectric interaction is present in the magnetic layers ( $\alpha = 0$ ), and the dotted lines refer to the case when the magnetolectric coupling is taken into account with  $\alpha = 30 \text{ ps m}^{-1}$ . The subpeak number is the same in each mode in the  $T_{pp}$  and  $T_{ss}$  spectra [blue and green lines

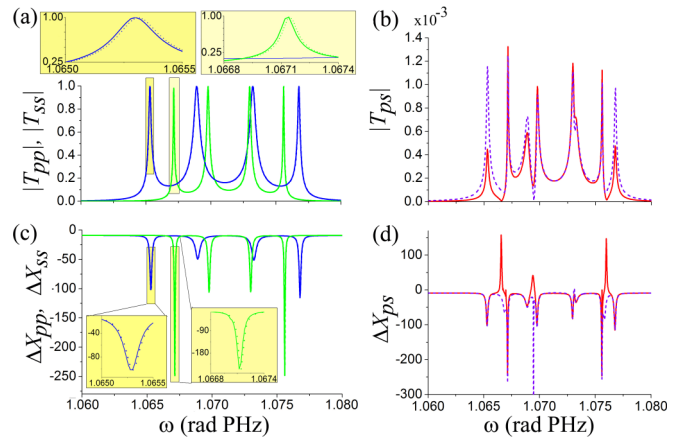


FIG. 6. Fine structure of the inside-band-gap modes in (a)  $|T_{pp}|$  (blue lines) and  $|T_{ss}|$  (green lines); (b)  $|T_{ps}|$ ; (c)  $\Delta X_{pp}$  (blue lines) and  $\Delta X_{ss}$  (green lines); (d)  $\Delta X_{ps}$  for  $\theta = 30^\circ$  and the structure  $[M(AB)^4A]^5M$  in the cases when the magnetolectric constant  $\alpha = 0$  (solid lines) and  $\alpha = 30 \text{ ps m}^{-1}$  (dotted lines).

in Fig. 6(a)], but it differs from that in the  $T_{ps}$  spectrum [Fig. 6(b)]. The frequency positions of the subpeaks of  $T_{pp}$  and  $T_{ss}$  are different but overlap with those of  $T_{ps}$  [Figs. 6(a) and 6(b)]. The inside-band-gap mode widths in  $T_{pp}$  and  $T_{ps}$  spectra ( $\Delta w_{pp,ps} \approx 17$  rad THz) are larger than that in the  $T_{ss}$  spectrum ( $\Delta w_{ss} \approx 10$  rad THz).

The GHSs demonstrate the same fine structure, and the frequency positions of the subpeaks of  $\Delta X_{ij}$  coincide with those of  $T_{ij}$ , as shown in Figs. 6(c) and 6(d). As was mentioned above,  $\Delta X_{ps}$  can be as negative as it is positive, when no magnetoelectric interaction is present in the magnetic layers [solid line in Fig. 6(d)], on the contrary to always-negative  $\Delta X_{pp}$  and  $\Delta X_{ss}$ . Positions of the positive maxima of  $\Delta X_{ps}$  correspond to the position of the gaps between the subpeaks of  $T_{ps}$  [solid lines in Figs. 6(b) and 6(d)]. However, not every gap in  $T_{ps}$  is accompanied by  $\Delta X_{ps} > 0$ . For instance, in the middle of the inside-band-gap mode (at  $\omega \approx 1.072$  rad PHz), a smooth change of  $T_{ps}$  does not result in large variations of its phase and does not produce a GHS peak.

As one can see from comparison of the solid and dotted lines in the insets in Figs. 6(a) and 6(c), the linear magnetoelectric interaction leads to a slight shift of  $T_{pp}$  and  $T_{ss}$  and the corresponding GHSs  $\Delta X_{pp}$  and  $\Delta X_{ss}$  towards higher frequencies. However, this shift is only of about 0.02 rad THz. On the contrary, magnetoelectric interaction results in the increase of  $T_{ps}$  at low- and high-frequency subpeaks of the inside-band-gap mode and in a slight modification of the other subpeaks [Fig. 6(b)]. This, in turn, through modification of  $T_{ps}$  leads to causing the positive maxima of  $\Delta X_{ps}$  to disappear, so the GHS becomes negative in all frequency ranges [dotted line in Fig. 6(d)].

#### IV. CONCLUSION

In conclusion, we analyzed theoretically the Goos-Hänchen effect of the near-infrared electromagnetic beams in biperiodic photonic-magnonic crystals and showed a modification of the lateral shift of the transmitted Gaussian wave packet for all polarization states of the incident and transmitted beams. We showed the increase of the Goos-Hänchen shift at the frequencies of the inside-photonic-band-gap modes and enhancement of the shift peaks due to the linear magnetoelectric effect in the magnetic layers for the case of a  $p$ - ( $s$ -) polarized transmitted beam produced by an  $s$ - ( $p$ -) polarized incident beam. As shown in a recent paper [67], a modern experimental setup allows providing measurements with high accuracy for different polarization combinations even for a relatively weak signal. We hope that the results of our analysis of the Goos-Hänchen effect in biperiodic photonic-magnonic crystals will be useful for the future investigation of complex multiperiodic photonic structures.

#### ACKNOWLEDGMENTS

This research is supported by the Ministry of Education and Science of the Russian Federation (Project No. 14.Z50.31.0015 and State Contract No. 3.7614.2017/П220), the Russian Science Foundation (Project No. 15-19-10036), the European Union's Horizon 2020 research and innovation program under the Marie Skłodowska-Curie Grant No. 644348, and the Ukrainian State Fund for Fundamental Research (Project No. Ф71/59-2017).

- 
- [1] F. Goos and H. Hänchen, *Ann. Phys.* **436**, 333 (1947).
  - [2] S. Asiri, J. Xu, M. Al-Amri, and M. S. Zubairy, *Phys. Rev. A* **93**, 013821 (2016).
  - [3] M. P. Araujo, S. De Leo, and G. G. Maia, *Phys. Rev. A* **93**, 023801 (2016).
  - [4] S. Chen, C. Mi, L. Cai, M. Lin, H. Luo, and S. Wen, *Appl. Phys. Lett.* **110**, 031105 (2017).
  - [5] M. Abbas, Ziauddin, and S. Qamar, *J. Opt. Soc. Am. B* **34**, 245 (2017).
  - [6] P. K. Swain, N. Goswami, and A. Saha, *Opt. Commun.* **382**, 1 (2017).
  - [7] L. Lambrechts, V. Ginis, J. Danckaert, and P. Tassin, *Phys. Rev. B* **95**, 035427 (2017).
  - [8] R. Macêdo and T. Dumelow, *J. Opt.* **15**, 014013 (2013).
  - [9] I. J. Singh and V. P. Nayyar, *J. Appl. Phys.* **69**, 7820 (1991).
  - [10] S. B. Borisov, N. N. Dadoenkova, I. L. Lyubchanskii, and M. I. Lyubchanskii, *Opt. Spectrosc.* **85**, 225 (1998).
  - [11] F. Lima, T. Dumelow, E. L. Albuquerque, and J. A. P. da Costa, *Phys. Rev. B* **79**, 155124 (2009).
  - [12] T. Tang, J. Qin, J. Xie, L. Deng, and L. Bi, *Opt. Express* **22**, 27042 (2014).
  - [13] R. Macêdo, R. L. Stamps, and T. Dumelow, *Opt. Express* **22**, 28467 (2014).
  - [14] Yu. S. Dadoenkova, F. F. L. Bentivegna, N. N. Dadoenkova, I. L. Lyubchanskii, and Y. P. Lee, *J. Opt. Soc. Am. B* **33**, 393 (2016).
  - [15] Yu. S. Dadoenkova, F. F. L. Bentivegna, N. N. Dadoenkova, R. V. Petrov, I. L. Lyubchanskii, and M. I. Bichurin, *J. Appl. Phys.* **119**, 203101 (2016).
  - [16] W. Yu, H. Sun, and L. Gao, *Sci. Rep.* **7**, 45866 (2017).
  - [17] Y. Fan, N.-H. Shen, F. Zhang, Z. Wei, H. Li, Q. Zhao, Q. Fu, P. Zhang, T. Koschny, and C. M. Soukoulis, *Adv. Opt. Mater.* **4**, 1824 (2016).
  - [18] M. Merano, *Opt. Lett.* **41**, 5780 (2016).
  - [19] S. Grosche, A. Szameit, and M. Ornigotti, *Phys. Rev. A* **94**, 063831 (2016).
  - [20] Yu. S. Dadoenkova, N. N. Dadoenkova, I. L. Lyubchanskii, and Y. P. Lee, *J. Appl. Phys.* **118**, 213101 (2015).
  - [21] Yu. S. Dadoenkova, N. N. Dadoenkova, I. L. Lyubchanskii, Y. P. Lee, and Th. Rasing, *Photonics Nanostruct.* **11**, 345 (2013).
  - [22] D. Felbacq, A. Moreau, and R. Smaïli, *Opt. Lett.* **28**, 1633 (2003).
  - [23] J. Hu, B. Liang, J. Chen, X. Cai, Q. Jiang, and S. Zhuang, *J. Opt.* **18**, 075103 (2016).
  - [24] I. V. Soboleva, V. V. Moskalenko, and A. A. Fedyanin, *Phys. Rev. Lett.* **108**, 123901 (2012).
  - [25] Q. Jiang, J. Chen, B. Liang, Y. Wang, J. Hu, and S. Zhuang, *Opt. Lett.* **42**, 1213 (2017).
  - [26] A. Aiello, *New J. Phys.* **14**, 013058 (2012).
  - [27] K. Y. Bliokh and A. Aiello, *J. Opt.* **15**, 014001 (2013).

- [28] Ziauddin, Y.-L. Chuang, S. Quamar, and R.-K. Lee, *Sci. Rep.* **6**, 26504 (2016).
- [29] V. J. Vallapragada, A. P. Ravishankar, G. L. Mulay, G. S. Agarwal, and V. G. Achanta, *Sci. Rep.* **6**, 19319 (2016).
- [30] Yu. S. Dadoenkova, N. N. Dadoenkova, I. L. Lyubchanskii, M. Sokolovskyy, J. W. Klos, J. Romero-Vivas, and M. Krawczyk, *Appl. Phys. Lett.* **101**, 042404 (2012).
- [31] P. Gruszecki, J. Romero-Vivas, Yu. S. Dadoenkova, N. N. Dadoenkova, I. L. Lyubchanskii, and M. Krawczyk, *Appl. Phys. Lett.* **105**, 242406 (2014).
- [32] P. Gruszecki, Yu. S. Dadoenkova, N. N. Dadoenkova, I. L. Lyubchanskii, J. Romero-Vivas, K. Y. Guslienko, and M. Krawczyk, *Phys. Rev. B* **92**, 054427 (2015).
- [33] P. Gruszecki, M. Mailyan, O. Gorobets, and M. Krawczyk, *Phys. Rev. B* **95**, 014421 (2017).
- [34] D. Villegas, J. Appiagi, F. de Leon-Perez, and R. Perez-Alvarez, *J. Phys.: Condens. Matter* **29**, 125301 (2017).
- [35] Y. Nie, Y. Li, Z. Wu, X. Wang, W. Yuan, and M. Sang, *Opt. Express* **22**, 8943 (2014).
- [36] J. Sun, X. Wang, C. Yin, P. Xiao, H. Li, and Z. Cao, *J. Appl. Phys.* **112**, 83104 (2012).
- [37] T. Tang, C. Li, L. Luo, Y. Zhang, and J. Li, *Appl. Phys. B* **122**, 167 (2016).
- [38] Z. Tahmasebi and M. Amiri, *Phys. Rev. A* **93**, 043824 (2016).
- [39] Yu. S. Dadoenkova, F. F. L. Bentivegna, V. V. Svetukhin, A. V. Zhukov, R. V. Petrov, and M. I. Bichurin, *Appl. Phys. B* **123**, 107 (2017).
- [40] Y. Wan, Z. Zheng, W. Kong, Y. Liu, Z. Lu, and Y. Bian, *Opt. Lett.* **36**, 3539 (2011).
- [41] A. Matthews and Yu. Kivshar, *Phys. Lett. A* **372**, 3098 (2008).
- [42] A. Madani and S. R. Entezar, *Superlattices Microstruct.* **86**, 105 (2015).
- [43] L. Wang and S. Zhu, *Appl. Phys. B* **98**, 459 (2010).
- [44] I. V. Shadrivov, A. A. Sukhorukov, and Yu. S. Kivshar, *Appl. Phys. Lett.* **82**, 3820 (2003).
- [45] L.-G. Wang and S.-Y. Zhu, *Opt. Lett.* **31**, 101 (2006).
- [46] S. Longhi, G. Della Valle, and K. Staliunas, *Phys. Rev. A* **84**, 042119 (2011).
- [47] Ziauddin, Y.-L. Chuang, and R.-K. Lee, *Phys. Rev. A* **92**, 013815 (2015).
- [48] W. Klos, M. Krawczyk, Yu. S. Dadoenkova, N. N. Dadoenkova, and I. L. Lyubchanskii, *J. Appl. Phys.* **115**, 174311 (2014).
- [49] J. W. Klos, M. Krawczyk, Yu. S. Dadoenkova, N. N. Dadoenkova, and I. L. Lyubchanskii, *IEEE Trans. Magn.* **50**, 2504404 (2014).
- [50] Yu. S. Dadoenkova, N. N. Dadoenkova, I. L. Lyubchanskii, J. W. Klos, and M. Krawczyk, *J. Appl. Phys.* **120**, 073903 (2016).
- [51] E. E. Narimanov, *Phys. Rev. X* **4**, 041014 (2014).
- [52] T. H. O'Dell, *The Electrodynamics of Magnetolectric Media* (North Holland, Amsterdam, 1970).
- [53] B. B. Krichevtsov, V. V. Pavlov, R. V. Pisarev, and A. G. Selitsky, *Ferroelectrics* **161**, 65 (1994).
- [54] G. Winkler, *Magnetic Garnets* (Vieweg, Braunschweig, 1981).
- [55] Yu. S. Dadoenkova, I. L. Lyubchanskii, Y.P. Lee, and Th. Rasing, *Eur. Phys. J. B* **71**, 401 (2009).
- [56] Yu. S. Dadoenkova, I. L. Lyubchanskii, Y.P. Lee, and Th. Rasing, *Low Temp. Phys.* **36**, 538 (2010).
- [57] Yu. S. Dadoenkova, I. L. Lyubchanskii, Y.P. Lee, and Th. Rasing, *J. Opt. Soc. Am. B* **31**, 626 (2014).
- [58] R. R. Birss, *Symmetry and Magnetism* (North Holland, Amsterdam, 1966).
- [59] A. G. Gurevich and G. V. Melkov, *Magnetization Oscillations and Waves* (CRC Press, Boca Raton, FL, 1996).
- [60] D. W. Berreman, *J. Opt. Soc. Am.* **62**, 502 (1972).
- [61] S. B. Borisov, N. N. Dadoenkova, and I. L. Lyubchanskii, *Opt. Spectrosc.* **74**, 670 (1993).
- [62] K. Artmann, *Ann. Phys. (Leipzig, Ger.)* **1-2**, 87 (1948).
- [63] J. B. Goette and M. R. Dennis, *Opt. Lett.* **38**, 2295 (2013).
- [64] E. D. Palik, *Handbook of Optical Constants of Solids. Magnetic and Other Properties of Oxides and Related Compounds* (Academic Press, New York, 1991).
- [65] Landolt-Börnstein, in *Magnetic and Other Properties of Oxides and Related Compounds: Garnets and Perovskites, New Series*, Group III, Vol. 12, Pt. A, edited by K.-H. Hellwege and A. M. Hellwege (Springer, Berlin, 1978).
- [66] M. Torfeh and H. Le Gall, *Phys. Status Solidi A* **63**, 247 (1981).
- [67] V. J. Yallapragada, G. L. Mulay, C. N. Rao, A. P. Ravishankar, and V. G. Achanta, *Rev. Sci. Instrum.* **87**, 103109 (2016).